USB Proceedings

2014 International Conference on Electrical Machines (ICEM)

Andel`s Hotel Berlin
Berlin, Germany
02 - 05 September, 2014

Sponsored by

The Institute of Electrical and Electronics Engineers (IEEE)
IEEE Industrial Electronics Society (IES)

Co-sponsored by

ETG - Power Engineering Society withing VDI

A robust model reference adaptive controller for the PMSM drive system with torque estimation and compensation

Qian Liu, Andreas Thul and Kay Hameyer

***Abstract*—This paper focuses on a robustness controller and the performance of a permanent magnet synchronous machine (PMSM) with parameter uncertainty. The proposed controller is composed by a model reference adaptive current controller and a torque compensator. An internal model of the PMSM is introduced to define the transient reference behavior of the current and torque. A simple adaptation rule of the model uncertainty based on the Lyapunov theory and Symmetrical Optimum is given. With this approach the performance of the current controller and uncertainty estimation are guaranteed. For the torque estimation, the minimum switching time and the harmonics of the converter as well as the zero order hold in measurement result in steady state estimation error. In this paper, a torque estimator is given to compensate the mentioned torque error. In the end, the simulation results demonstrate the performance of the adaptive controller and the torque estimator.**

***Index Terms*—Robust adaptive control, robustness, permanent magnet synchronous machine, torque estimation, torque ripple, parameter variation, digital implementation.**

I. Introduction

Currently in electrical vehicles and various industry applications, the permanent magnet synchronous machine (PMSM) is widely used in the drive system. This is due to its high power density, high efficiency and good controllability. With the appearance of the power electronic devices, several control strategies are invented with different purposes. The field oriented control (FOC) with PI controller and voltage modulation (PWM or SVM) is very popular in industry applications due to its simple structure and low cost implementation. As an alternative, the direct torque control (DTC) is introduced to achieve a fast torque response [1]. Recently the model predictive control (MPC) is introduced to obtain an optimal performance of the entire drive system with PMSM and the power converter [2] [3]. The mentioned controllers are designed based on a given reference model of the PMSM. The error and uncertainty in the machine model lead to deterioration of the dynamic performance and even yield instability when the controller is not properly designed.

On the other hand, one of the main disadvantages of the PMSM is the nonuniformity in the developed torque, i.e., the torque ripple [4]. The torque ripple of the PMSM is produced by the high order harmonics in the air gap flux due to the inner geometry of permanent magnets, slots and also the flux deviation of the permanent magnets under load. Those high order harmonics are complicated to model for the base frequency of the PMSM, which is usually used for the controller design. The winding resistance of the PMSM varies with frequency and temperature, which can degrade the performance of the PMSM [5]. Moreover, the pulse width modulator (SPWM or SVPWM) with limited switching frequency results in additional uncertainties in the PMSM drive system such as phase shift of the voltage [6] and voltage distortion [7].

In order to tolerate the model error and improve the dynamic performance of the PMSM drive system, an internal model control method (IMC) is coupled to the PI controller in an early stage. The IMC is relatively insensitive for model errors with a properly designed bandwidth. However, this results in undesired oscillation and the robustness of this approach is limited [8]. Another popular method to improve the robustness of the PMSM drive system is to design a nonlinear adaptive controller. In some references, the self-tuning adaptive controller is implemented with on-line parameter identification using extended Kalman filter (EKF) and recursive least squares (RLS) [9] [10]. This adaptive controller is very robust concerning the parameter errors. However, it is computational expensive due to the numerical RLS solution of the EKF. To reduce the computational cost of the controller, the parameter error of the PMSM is modeled as voltage uncertainty in the decoupled d and q axis respectively [11] [12] [13]. The controller design based on this single voltage uncertainty guarantees high robustness at low computational cost.

The torque error including the torque ripple caused by the model imperfection is usually estimated by the sliding mode observer [14] or the self-adaptation in the adaptive controller [11]. The comparison between the method of estimation is made in [15]. The self-adaptation torque estimation is now widely used due to its simple structure, high accuracy and relatively low computational cost. The estimated torque is compensated to minimize the steady state error and also the torque ripple to obtain a better performance for the PMSM.

In this paper, a nonlinear model reference adaptive direct current controller to estimate the uncertainty and disturbance in the machine model is proposed. The adaptive controller is designed with a simple model error estimator based on the combination of the Lyapunov and the linear control theory. The controller parameters are given both for the continuous and discrete implementation, with which the stability and performance of the proposed adaptive controller are guaranteed. On the other hand, due to the discretization of the digital microcontroller and the switching of the converter, errors for the torque. In this paper, a self-adaptation torque estimator is introduced to reduce the torque estimation error and the torque ripple caused by the model error.

978-1-4799-4775-1/14/$31.00 ©2014 IEEE

Qian.Liu@iem.rwth-aachen.de).

Prof. Kay Hamayer is the director of Institute of Electrical Machines (IEM) at RWTH Aachen University.

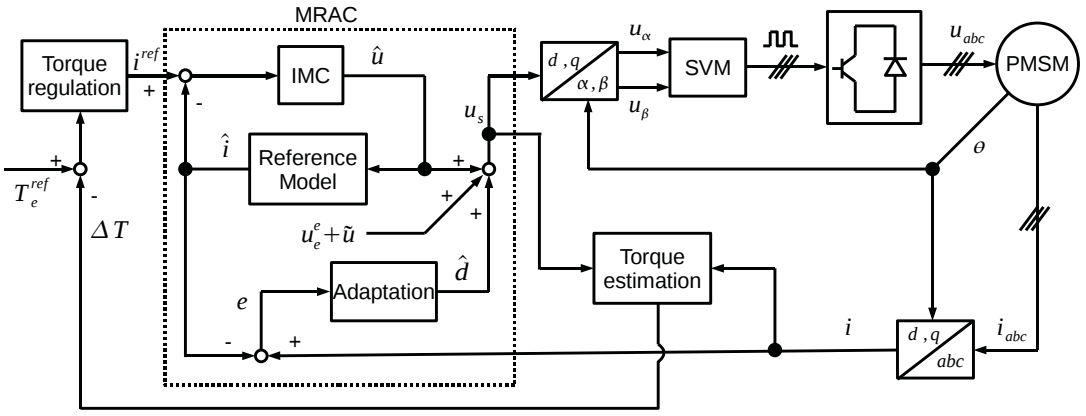

Fig. 1. Proposed adaptive control structure of the PMSM.

II. Model of a PMSM

With the idea of the vector control of an AC machine, the model of a PMSM can be presented in the synchronous rotational coordinate reference frame with DC quantities. The 2-axis model of a PMSM is shown by the following equations (1) and (2) using power invariant transformation:

$$u_d = Ri_d + L_d\frac{di_d}{dt} - \omega L_q i_q + \epsilon_d \tag{1}$$

$$u_q = Ri_q + L_q\frac{di_q}{dt} + \omega(L_d i_d + \psi_F) + \epsilon_q \tag{2}$$

$$T_e = p(\psi_F + (L_d - L_q)i_d)i_q \tag{3}$$

where R, L_d and L_q are the stator resistance and inductances of the PMSM. ψ_F is the magnetic flux of the permanent magnets. p is the pole pair number. ϵ_d and ϵ_q are the unmodeled uncertainties, which include the high order harmonic dynamics of the PMSM, environment disturbance and the influence of the PWM voltage source.

In different operating points, the machine parameters R, L_d, L_q and ψ_F are changing due to the environment temperature and load condition, which deteriorates the transient performance of the PMSM. In order to simplify the machine model for the controller design, equations (1) and (2) are transformed into the state space expression and all the parameter displacement and unmodeled uncertainties can be integrated into two variables [11] [12], which are shown by (4):

$$\dot{\boldsymbol{i}} = \boldsymbol{A_0 i} + \boldsymbol{B_0}(\boldsymbol{u_s} + \boldsymbol{u_e} - \boldsymbol{d}) \tag{4}$$

where the vectors and matrix in (4) are defined as:

$$\boldsymbol{i} = \begin{bmatrix} i_d \\ i_q \end{bmatrix} \quad \boldsymbol{u_s} = \begin{bmatrix} u_d \\ u_q \end{bmatrix} \quad \boldsymbol{u_e} = \begin{bmatrix} \omega L_q i_q \\ -\omega(L_d i_d + \psi_{F0}) \end{bmatrix}$$

$$\boldsymbol{d} = \begin{bmatrix} d_d \\ d_q \end{bmatrix} \quad \boldsymbol{A_0} = \begin{bmatrix} -\frac{R_0}{L_{d0}} & 0 \\ 0 & -\frac{R_0}{L_{q0}} \end{bmatrix} \quad \boldsymbol{B_0} = \begin{bmatrix} \frac{1}{L_{d0}} & 0 \\ 0 & \frac{1}{L_{q0}} \end{bmatrix}$$

here R_0, L_{d0}, L_{q0} and ψ_{F0} are the constant reference values for the PMSM parameters, which are usually obtained by the no load and locked rotor test. The vector $\boldsymbol{d}$ is the total model error and disturbance decomposed in d and q axis, which is operating point dependent and unmeasurable. The detailed

all the unknown issues are integrated into the vector $\boldsymbol{d}$, the model (4) describes the transient behavior of the PMSM without loss of generality.

III. Model reference adaptive current control of the PMSM

The model reference adaptive controller (MRAC) regulates the system to be performed in terms of a pre-defined reference system. Therefore, the MRAC is more convenient to give a desired transient response to the objective system when compared to the self-tunning adaptive controller [16]. Fig. 1 shows the structure of the proposed controller for the PMSM. The part enclosed by the dotted line is the model reference adaptive current controller. The designed IMC regulates the reference model to generate the desired transient response of the current for the PMSM. Meanwhile, the adaptation process adapts the model error and guarantees the current transient response of the PMSM, which will be discussed on the following sections.

A. Reference model and IMC of the PMSM

The reference model of the PMSM in d-q coordinates, which has the same structure of the PMSM in (4), is an ideal base frequency model without any uncertainty. The reference model is shown by the following equations:

$$\dot{\hat{\boldsymbol{i}}} = \boldsymbol{A_0}\hat{\boldsymbol{i}} + \boldsymbol{B_0}(\hat{\boldsymbol{u}} + \hat{\boldsymbol{u}}_{\boldsymbol{e}}) \tag{5}$$

where $\boldsymbol{A_0}$ and $\boldsymbol{B_0}$ are defined in the last section. $\hat{\boldsymbol{i}}$ and $\hat{\boldsymbol{u}}$ are the current and terminal voltage vectors of the reference model respectively. $\hat{\boldsymbol{u}}_{\boldsymbol{e}}$ is the back-emf voltage which is defined as: $\hat{\boldsymbol{u}}_{\boldsymbol{e}} = [\omega L_{q0}\hat{i}_q - \omega(L_{d0}\hat{i}_d + \psi_{F0})]^T$. The superscript T means the transpose of a matrix.

Since the reference model is already deterministic, a decoupled IMC is introduced. The detailed description of the decoupled IMC can be found in [8]. The reference voltage $\hat{\boldsymbol{u}}$ is obtained by (6):

$$\hat{\boldsymbol{u}} = \frac{1}{T_{imc}}\boldsymbol{B_0}^{-1}\hat{\boldsymbol{e}} + \frac{1}{T_{imc}}\boldsymbol{B_0}^{-1}\boldsymbol{A_0}\int \hat{\boldsymbol{e}}dt - \hat{\boldsymbol{u}}_{\boldsymbol{e}} \tag{6}$$

where the error signal $\hat{\boldsymbol{e}}$ is defined as $\hat{\boldsymbol{e}} = \boldsymbol{i}_{ref} - \hat{\boldsymbol{i}}$. And T_{imc} is a time constant, which can be any positive value. According to (6), the entire system including reference model and IMC performs as a low pass filter with the following transfer function:

Therefore, the transient response of $\hat{\boldsymbol{i}}$ has no overshot and its rising time is simply determined by the time constant

T_{imc}. For its digital implementation, the time constant T_{imc} should be chosen to be larger than the sampling time.

B. Adaptation of the model error and voltage

The adaptation process of the proposed controller is based on the error signal between the model and measured current. Using (4) - (5), the model error is described by the following system dynamics:

$$\dot{\boldsymbol{e}} = \boldsymbol{A_0 e} + \boldsymbol{B_0}(\boldsymbol{u_s} - \hat{\boldsymbol{u}} + \boldsymbol{u_e^e} - \boldsymbol{d}) \tag{8}$$

where the error signal vector $\boldsymbol{e}$ is defined as $\boldsymbol{e} = \boldsymbol{i} - \hat{\boldsymbol{i}}$. The emf error is denoted as $\boldsymbol{u_e^e} = [\omega L_{q0} e_q,\ -\omega L_{d0} e_d]^T$. Denote $\boldsymbol{u_s} = \tilde{\boldsymbol{u}} + \hat{\boldsymbol{u}} - \boldsymbol{u_e^e} + \hat{\boldsymbol{d}}$, where $\hat{\boldsymbol{d}}$ is an estimated value of the model error. Therefore, the equation (8) can be simplified by the following notation:

$$\dot{\boldsymbol{e}} = \boldsymbol{A_0 e} + \boldsymbol{B_0}(\tilde{\boldsymbol{u}} + \tilde{\boldsymbol{d}}) \tag{9}$$

where $\tilde{\boldsymbol{d}}$ is defined as the difference between the estimated and real model error with $\tilde{\boldsymbol{d}} = \hat{\boldsymbol{d}} - \boldsymbol{d}$.

To adapt the error $\tilde{\boldsymbol{d}}$ and voltage $\tilde{\boldsymbol{u}}$, the Lyapunov theory is applied. A quadratic Lyapunov function is defined by the following equation:

$$V = \frac{1}{2}(\boldsymbol{e^T e} + \tilde{\boldsymbol{d}}^{\boldsymbol{T}} \boldsymbol{\Lambda} \tilde{\boldsymbol{d}}) \tag{10}$$

where the matrix Λ is a positive definite diagonal matrix with diagonal element $\frac{1}{\Lambda_d}$ and $\frac{1}{\Lambda_q}$. Take the derivative of the Lyapunov function and substitute (9) into (10), we find

$$\begin{aligned} \dot{V} &= \dot{\boldsymbol{e}}^{\boldsymbol{T}} \boldsymbol{e} + \dot{\tilde{\boldsymbol{d}}}^{\boldsymbol{T}} \boldsymbol{\Lambda} \tilde{\boldsymbol{d}} \\ &= \boldsymbol{e^T}(\boldsymbol{A_0 e} + \boldsymbol{B_0}\tilde{\boldsymbol{u}}) + \tilde{\boldsymbol{d}}^{\boldsymbol{T}}(\boldsymbol{B_0^T e} + \boldsymbol{\Lambda}\dot{\tilde{\boldsymbol{d}}}) \end{aligned} \tag{11}$$

Choose the adaptation rule that

$$\tilde{\boldsymbol{u}} = -\boldsymbol{k_1 B_0^T e} \tag{12}$$

$$\dot{\tilde{\boldsymbol{d}}} = -\boldsymbol{\Lambda^{-1} B_0^T e} \tag{13}$$

where $\boldsymbol{k_1}$ is a positive definite diagonal matrix with diagonal elements k_{1d} and k_{1q}. With (12) and (13) the derivative of the Lyapunov function can be reformed into:

$$\dot{V} = \boldsymbol{e^T}(\boldsymbol{A_0} - \boldsymbol{B_0 k_1 B_0^T})\boldsymbol{e} \leq 0 \tag{14}$$

It is obvious that the derivative of the Lyapunov function $\dot{V}$ is less than or equal to zero, zero can only be reached when $\boldsymbol{e} = \boldsymbol{0}$. Therefore, the invariant set of the Lyapunov function V is $\{(\boldsymbol{e}, \tilde{\boldsymbol{d}}) : \boldsymbol{e} = \boldsymbol{0}\}$. On the other hand, equations (9), (12) and (13) indicate that when $\boldsymbol{e} = \boldsymbol{0}$, $\dot{\tilde{\boldsymbol{d}}} = \boldsymbol{0}$ also holds. According to the Lasalle's Invariant Set Theorem [17], the system (9) is globally asymptotically stable to the origin, which means that the current of the PMSM towards to the current of the reference model asymptotically.

C. Determination of the controller parameters

In order to choose appropriate controller parameters to guarantee the transient performance of the error signal, equations (12) and (13) are substituted into (9) and take the derivative. Then we have:

$$\boldsymbol{B_0^{-T} \Lambda B_0^{-1}} \ddot{\tilde{\boldsymbol{d}}} - (\boldsymbol{A_0} - k_1 \boldsymbol{B_0^T B_0}) \boldsymbol{\Lambda B_0^{-T} B_0^{-1}} \dot{\tilde{\boldsymbol{d}}} + \dot{\hat{\boldsymbol{d}}} = \dot{\boldsymbol{d}} \tag{24}$$

where (15) is a linear decoupled system in d,q coordinates in rotor fixed reference frame. Without loss of generality, the analysis of d-axis is illustrated. The d-axis system is described by the following equation:

$$\ddot{e}_d + (\frac{R_0}{L_{d0}} + \frac{k_{1d}}{L_{d0}^2})\dot{e}_d + \frac{\Lambda_d}{L_{d0}^2} e_d = 0 \tag{16}$$

From (16) it can be noticed that k_{1d} and Λ_d determine the raising time and overshot of the error signal e_d. For simple implementation and avoidance of the overshot, the poles of the transfer function are set to the the same real number with:

$$\Lambda_d = \frac{1}{4}(R_0 + \frac{k_{1d}}{L_{d0}})^2 \tag{17}$$

so that the closed loop system for (17) is:

$$G_d(s) = \frac{1}{[s + \frac{1}{2L_{d0}}(R_0 + \frac{k_{1d}}{L_{d0}})]^2} \tag{18}$$

where s is the Laplace operator. The parameter k_{1d} can be easily designed to fit the rising time and frequency band of the error signal e_d.

For the digital implementation, the Euler forward discretization of the continuous system (16) is applied with $\dot{x} = \frac{x_{k+1} - x_k}{T_s}$. T_s is the sampling time. The discrete model of the d-axis system is:

$$\begin{aligned} e_{k+2} &+ [T_s(\frac{R_0}{L_{d0}} + \frac{k_{1d}}{L_{d0}^2}) - 2]e_{k+1} \\ &+ [1 - T_s(\frac{R_0}{L_{d0}} + \frac{k_{1d}}{L_{d0}^2}) + \frac{T_s^2 \Lambda_d}{L_{d0}^2}]e_k = 0 \end{aligned} \tag{19}$$

Choose Λ_d also by the equation (17), The discrete transfer function for the d-axis system is:

$$G_d(z) = \frac{1}{[z + \frac{T_s}{2L_{d0}}(R_0 + \frac{k_{1d}}{L_{d0}}) - 1]^2} \tag{20}$$

where z is the operator for the z-transformation. To guarantee the stability of the discrete system (20) and to avoid the sign reverse, the following limitation for k_{1d} must be fulfilled:

$$-1 < \frac{T_s}{2L_{d0}}(R_0 + \frac{k_{1d}}{L_{d0}}) - 1 < 0 \tag{21}$$

The convergence rate of (20) can be determined by k_{1d}. Similarly, for the q-axis in (15), the parameter Λ_q is chosen as:

$$\Lambda_q = \frac{1}{4}(R_0 + \frac{k_{1q}}{L_{q0}})^2 \tag{22}$$

and for the digital implementation, the following limitation holds:

$$-1 < \frac{T_s}{2L_{q0}}(R_0 + \frac{k_{1q}}{L_{q0}}) - 1 < 0 \tag{23}$$

Therefore, the matrix $\boldsymbol{\Lambda}$ is defined by equations (17) and (22) to guarantee the transient performance. Besides for the digital implementation, the parameter $\boldsymbol{k_1}$ is limited by both (21) and (23).

D. Estimation of the model error

The model error $\boldsymbol{d}$ is estimated by the classic symmetrical optimum method for a linear system. Using (8), (12)

Here the d-axis is again shown as an example with the following differential equation from (24):

$$\frac{L_{d0}^2}{\Lambda_d}[\dddot{\hat{d}}_d - (\frac{R_0}{L_{d0}} - \frac{k_1}{L_{d0}^2})\ddot{\hat{d}}_d] + \dot{\hat{d}}_d = d_d \qquad (25)$$

Equation (25) is a typical symmetric optimum problem, where $\hat{d}_d$ can be considered as the control unit and d_d is the system disturbance.

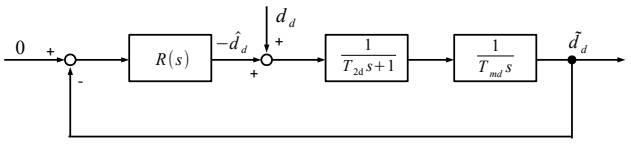

Fig. 2. Estimation of the model error with structure of symmetric optimum.

Fig. 2 shows the estimation structure for the model error estimation, where $R(s)$ is the estimator. T_{2d} and T_{md} are two time constants which are defined by:

$$T_{2d} = \frac{1}{\frac{R_0}{L_{d0}} + \frac{k_{1d}}{L_{d0}^2}} \qquad (26)$$

$$T_{md} = L_{d0}^2 \frac{1}{\Lambda_d T_{2d}} \qquad (27)$$

According to the principle of the symmetric optimum, the structure of $R(s)$ is shown by equation (28).

$$R(s) = \frac{V_d}{T_{id}s} + V_d \qquad (28)$$

$$T_{id} = a^2 T_{2d} \qquad V_d = \frac{T_{md}}{aT_{2d}}$$

where a is a positive real number which is larger than 1. Similarly, the model error d_q in q-axis can be also estimated by using the same estimator (28) but with different parameters. For the digital implementation, an discrete integration is utilized instead of the continuous one in (28). The symmetric optimum performs well with unknown system disturbance and has no steady state error [18] The estimated value $\hat{\boldsymbol{d}}$ converges towards the model error $\boldsymbol{d}$ with guaranteed transient performance. It should be noticed that the time constants based on k_1 and a of the adaptation process should be much smaller than the time constant T_{imc} of the IMC since the adaptation process is considered as a fast inner loop for the proposed control approach.

IV. Torque estimation and compensation

According to (3), the parameter error of the PMSM results in torque displacement. In [11] and [14] a torque estimation with d-axis flux and q-axis current are implemented. The d-axis flux is obtained by the division of the voltage and rotational speed. With this idea, the torque displacement can be calculated by (29)

$$\Delta T = \frac{p\hat{d}_q i_q}{\omega} \qquad (29)$$

However, the estimated model error $\hat{d}_q$ does not only consist of the parameter error of the PMSM, but also on distortion. The phase shift caused by the SVM, the turn on/off time and voltage distortion of the converter results in steady state error to the estimated torque displacement when (29) is applied. Therefore the influence of the converter should be removed from $\hat{d}_q$. Since the turn on/off time of the IGBT converter is usually less than 1 μs, which is much smaller than the switching time of the IGBT converter (switching frequency up to 20 kHz), the influence of the turn on/off time can be neglected. It is complicated to determine the voltage distortion due to nonideal IGBT. It is not considered in this paper. On the other hand, for the SVM, denote $T_c = \frac{1}{f_c}$ as the sampling time of the converter, where f_c is the frequency of the triangle signal. Due to the modulation strategy, the calculated duty circle for each IGBT is sampled with sampling frequency f_c. Therefore, a phase shift of the voltage with delay time $\frac{T_c}{2}$ exits after modulation. Besides, the delay due to the calculation of the digital processor is one sampling time T_c. These should be considered for the torque displacement estimation.

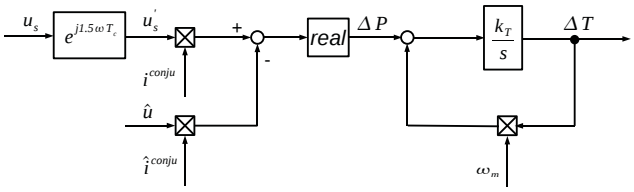

Fig. 3. Structure of the torque estimator.

Fig. 3 shows the structure of the proposed torque displacement estimator. The phase shift $1.5\omega T_c$ is compensated. $\omega_m = \frac{\omega}{p}$ is the mechanical rotational speed of the machine. The active power displacement $\Delta P = \omega_m \Delta T$ is estimated. To avoid the division by ω_m, which is very sensitive to the measurement noise at low speed operation, an integration estimator is introduced instead. It can be noticed that the integration estimator also behaves as a low pass filter with speed dependent frequency band $k_T\omega_m$. In order to compensate the cogging torque which is dominated by the sixth harmonic flux component of the permanent magnets and the torque ripple caused by the first and second current harmonics [14], $k_T = 6p$ in fig. 3 is proposed.

V. Simulation results

The simulations are performed in Matlab/Simulink with the structure from fig.1. The sampling frequency of the converter and the measurements are 10 kHz. The converter and the PMSM are simulated as continuous system, which current and speed are measured by zero-order-holder with the sampling frequency. Meanwhile the control part is implemented as digital controller with sampled measurement and a symmetric SVM is applied. The converter is modeled as an ideal switch with 1 μs turn on/off time. A PMSM with following parameters is used for the simulation: $p = 4$, $R_0 = 0.2\,\Omega$, $L_{d0} = L_{q0} = 5\,\mathrm{mH}$ and $\psi_{F0} = 0.3485\,\mathrm{Vs}$. The time constant of the IMC is set to $T_{imc} = 0.01\,\mathrm{s}$. The mechanical load torque is simulated with $T_m = k_m\omega_m$.

The reference torque is chosen to 20 Nm. The coefficient $k_m = 0.03\,\mathrm{Nms}$ is applied in such a way that the rotational speed of the PMSM will increase to 1600 rpm. The PMSM with $T_{imc} = 0.015$) to compare to the proposed adaptive controller. The delay T_c due to the calculation of digital processor is not considered in the simulation.

At first the simulation is made without PMSM parameter error. In this simulation, the torque compensation in fig.1 is not implemented. In this condition, the PI controller has the same transient behavior as the proposed controller. Fig. 4 shows the current and torque response of the PMSM. Fig. 5 shows the estimated model error $\hat{d}_d$, $\hat{d}_q$ and torque displacement ΔT. It can be noticed that without PMSM parameter error, the model error still exists due to the voltage phase shift caused by the SVM and converter. A steady state error of the estimated torque displacement exists when equation (29) is applied, which proved the theoretical statement in the previous section. With the proposed estimator in fig. 3, the steady state error is eliminated. Therefore, the proposed torque displacement estimator is chosen for the rest of the simulations.

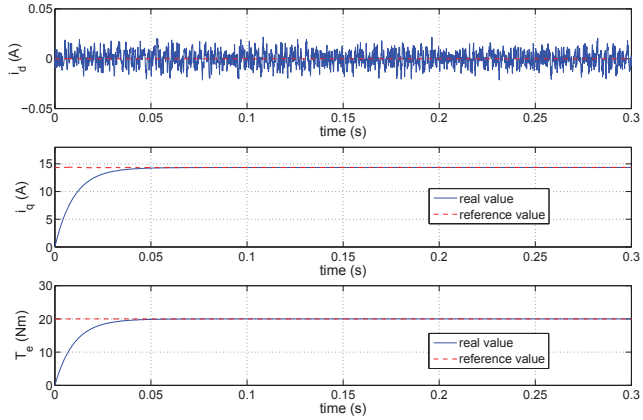

Fig. 4. Current and torque response of the proposed control scheme without parameter error and torque compensation.

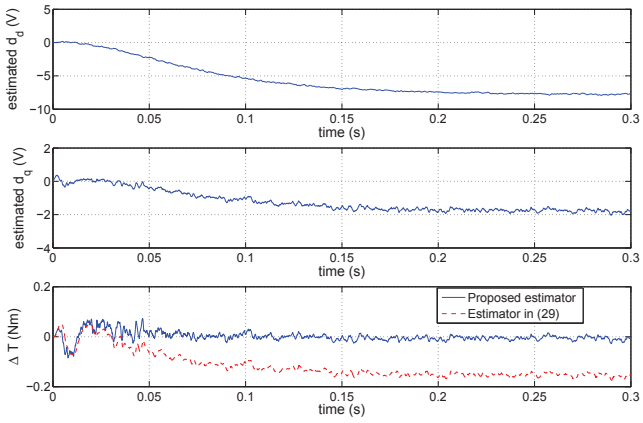

Fig. 5. Estimated model error and torque displacement for the proposed control scheme without parameter error and torque compensation.

In order to compare the performance of the PI to the proposed controller, in the following simulations, a sixth order flux harmonic component is inserted to the PMSM. The amplitude of the harmonic is calculated by using the method described in [19] with PM coverage factor of 0.9. The sixth harmonics in d- and q-axis are $\psi_{6d} = -0.032\cos(6\theta)$ Vs and $\psi_{6q} = 0.016\sin(6\theta)$ Vs.

Fig. 6 and Fig. 7 show the current and torque response of the proposed controller almost have no difference compared to the no error case in fig. 4. In contrast, the current and toque responses are slowed down when the PI controller is applied. On the other hand, the current harmonics is also smaller for the proposed controller. The torque ripple factor $\frac{T_{ripple}}{T_e}$ for the proposed controller is reduced to 0.16 when compared to 0.37 for the PI controller. A small steady state error of 0.08 Nm for the torque exists for the proposed controller due the model error caused by the resistance, which results in erroneous estimation of the torque displacement shown in fig. 8. This steady state torque error is very small for high speed operation but maybe critical for the low speed operation. However, this steady state torque error can be compensated by an additional resistance estimator.

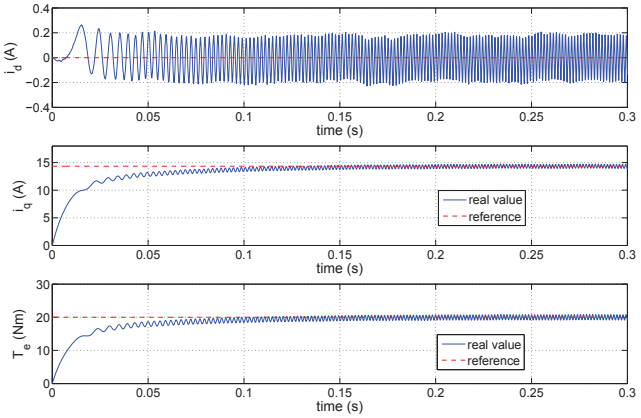

Fig. 6. Current and toque response with parameter error $R = 2R_0$ for the PI controller.

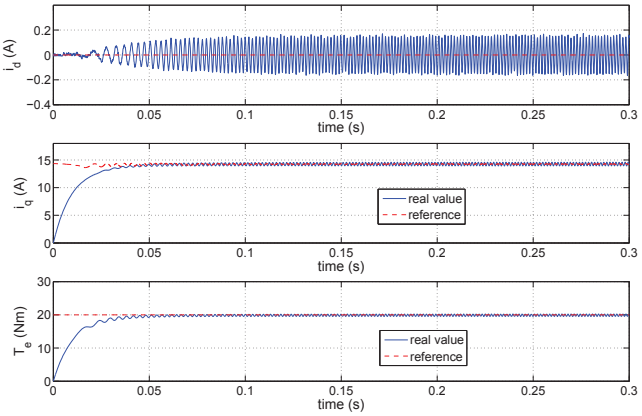

Fig. 7. Current and toque response with parameter error $R = 2R_0$ for the proposed controller.

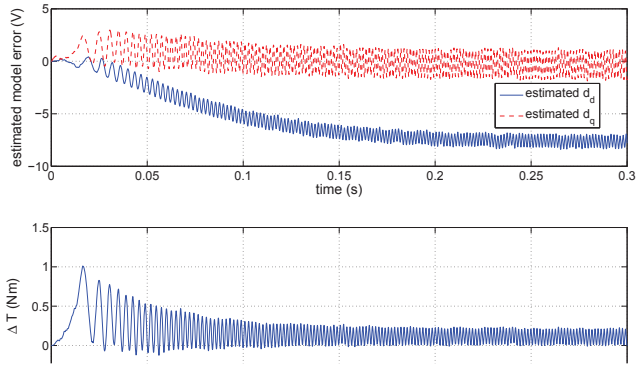

Fig. 8. Estimated model error and torque displacement for the proposed controller with $R = 2R_0$.

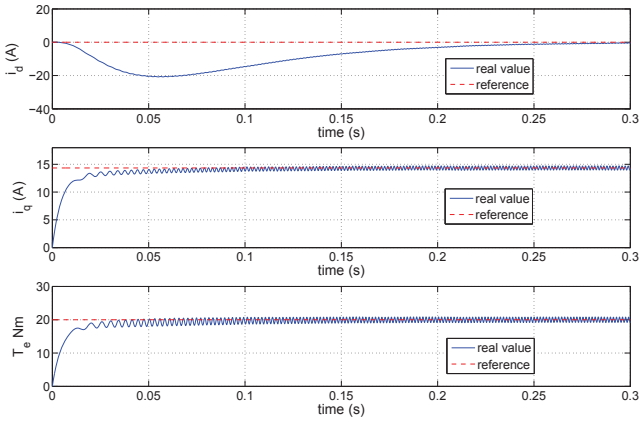

Fig. 9. Current and toque response with parameter error $L_q = 0.5L_{q0}$ for the PI controller.

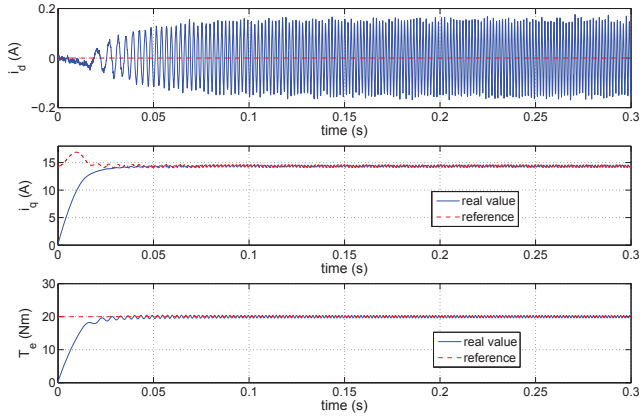

Fig. 10. Current and toque response with parameter error $L_q = 0.5L_{q0}$ for the proposed controller.

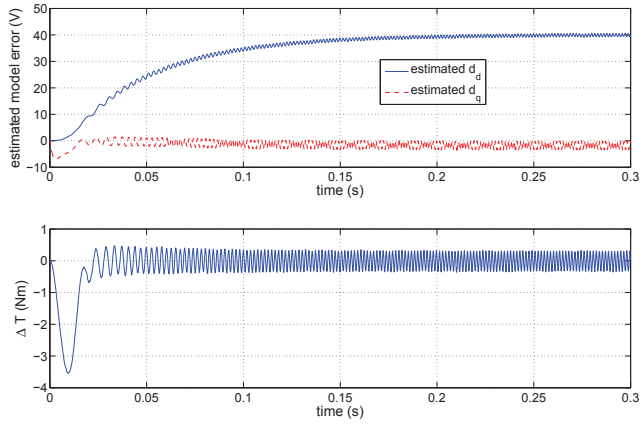

Fig. 11. Estimated model error and torque displacement for the proposed controller with $L_q = 0.5L_{q0}$.

Fig. 9 and Fig. 10 show the current and torque responses of the PMSM with parameter error $L_q = 0.5L_{q0}$ respectively. With a L_q error, there exists a large i_d overshot for the PI controller due to the imperfect decoupling, which can be tolerated for the proposed controller. The estimated model error $\hat{d}_d$ and $\hat{d}_q$ for the proposed controller converge fast and eliminate the influence of the model error. Therefore, PMSM performs approximately as the same as the reference model. Besides, the current harmonics are smaller for the proposed controller. The torque ripple factor for the proposed controller is reduced to 0.19 when compared to 0.4 of the PI controller. There is no steady state torque error. The parameter error $L_d = 0.5L_{d0}$ has a small influence on the performance of the PMSM for both PI and proposed controller, which is not shown here.

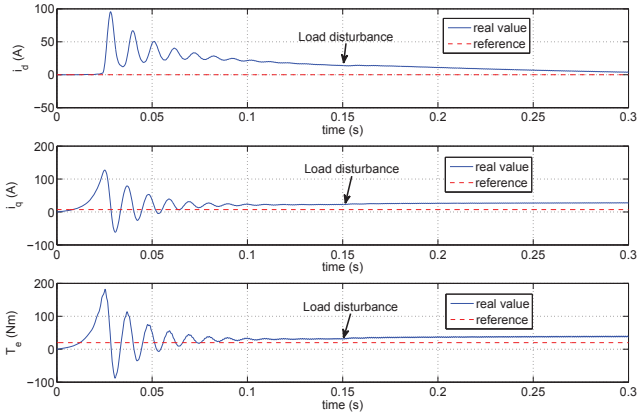

Fig. 12. Current and toque response with parameter error $\psi_F = 0.5\psi_{F0}$ for the PI controller.

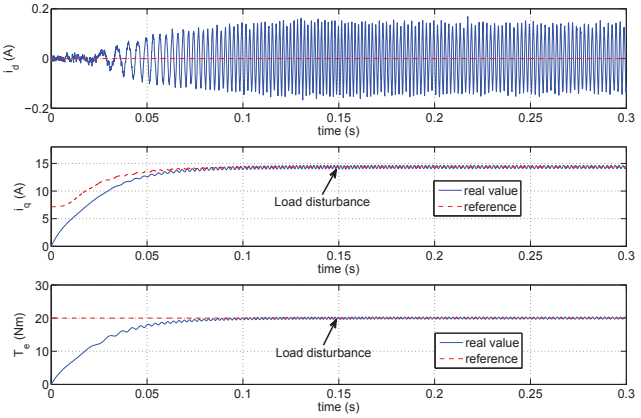

Fig. 13. Current and toque response with parameter error $\psi_F = 0.5\psi_{F0}$ for the proposed controller.

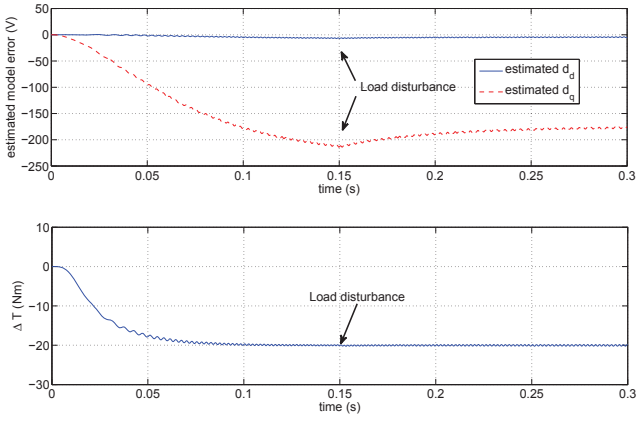

Fig. 14. Estimated model error and torque displacement for the proposed controller with $\psi_F = 0.5\psi_{F0}$.

Fig. 12 and fig. 13 show the performance for the PI and the proposed controller with parameter error $\psi_F = 0.5\psi_{F0}$ respectively. At the time $t = 0.15$s, a 5Nm load disturbance is imposed. For the PI controller, the imperfect decoupling caused by the flux error results in large oscillations in the current.

With the voltage limitation, the entire system is stabilized on the cost of a large steady state error in current and torque. For the proposed controller, the model error caused by the flux error is estimated (shown in fig. 14) and compensated to guarantee the transient performance of the current. The torque displacement between the reference model and the real PMSM shown in fig. 14, is compensated to generate an accurate current reference value. Therefore, there is no steady state torque error for the proposed controller with flux error. Besides, the load disturbance almost has no influence on the torque estimation and control due to the fast estimation of the model error.

Comparing the performance of the PMSM with and without parameter error, the parameter error has a small influence on the transient behavior for the PMSM with the proposed controller. The current and torque dynamics of the PMSM behave approximately in the same way as the desired reference system defined by (7).

VI. Conclusions

In this paper a model reference adaptive current controller with torque compensation is introduced, with which the PMSM can be operated approximately in the same way as the desired reference model. The proposed control scheme has a simple structure and is convenient for implementation. The stability of the MRAC with PMSM is theoretically proved by the Lyapunov theory. Meanwhile, the model error is estimated simply by the symmetric optimum method, with which the transient performance of the entire current loop can be analyzed and determined. The structure of a torque estimator is shown to eliminate the steady state torque estimation error caused by the phase shift of the SVM and converter. On the other hand, the torque estimator is designed to avoid the direct division of the speed, which may be sensitive to the measurement noise and disturbance. The simulation results show that the parameter error has a small influence on the PMSM with the proposed controller. The current harmonics and torque ripple can also be significantly reduced by the proposed controller.

References

[1] H. Zhu, X. Xiao, and Y. Li, "Torque ripple reduction of the torque predictive control scheme for permanent-magnet synchronous motors," *Industrial Electronics, IEEE Transactions on*, vol. 59, pp. 871–877, 2012.

[2] F. Morel, X. Lin-Shi, J.-M. Retif, B. Allard, and C. Buttay, "A comparative study of predictive current control schemes for a permanent-magnet synchronous machine drive," *Industrial Electronics, IEEE Transactions on*, vol. 56, pp. 2715–2728, 2009.

[3] S. Kouro, P. Cortes, R. Vargas, U. Ammann, and J. Rodriguez, "Model predictive control - a simple and powerful method to control power converters," *Industrial Electronics, IEEE Transactions on*, vol. 56, pp. 1826–1838, 2009.

[4] V. Petrovic, R. Ortega, A. Stankovic, and G. Tadmor, "Design and implementation of an adaptive controller for torque ripple minimization in pm synchronous motors," *Power Electronics, IEEE Transactions on*, vol. 15, pp. 871–880, 2000.

[5] D. Reigosa, P. Garcia, F. Briz, D. Raca, and R. Lorenz, "Modeling and adaptive decoupling of high-frequency resistance and temperature effects in carrier-based sensorless control of pm synchronous machines," *Industry Applications, IEEE Transactions on*, vol. 46, pp. 139–149, 2010.

[6] D. Mitchell, "Pulsewidth modulator phase shift," *Aerospace and Electronic Systems, IEEE Transactions on*, vol. AES-16, pp. 272–278,

estimation and compensation of pwm vsi for pmsm under resistance and flux linkage uncertainty," *Control Systems Technology, IEEE Transactions on*, vol. 14, pp. 589–601, 2006.

[8] L. Harnefors and H.-P. Nee, "Model-based current control of ac machines using the internal model control method," *Industry Applications, IEEE Transactions on*, vol. 34, pp. 133–141, 1998.

[9] S. Underwood and I. Husain, "Online parameter estimation and adaptive control of permanent-magnet synchronous machines," *Industrial Electronics, IEEE Transactions on*, vol. 57, pp. 2435–2443, 2010.

[10] L. Salvatore and S. Stasi, "Application of ekf to parameter and state estimation of pmsm drive," *Electric Power Applications, IEE Proceedings B*, vol. 139, pp. 155–164, 1992.

[11] Y. A. R. I. Mohamed, "A newly designed instantaneous-torque control of direct-drive pmsm servo actuator with improved torque estimation and control characteristics," *Industrial Electronics, IEEE Transactions on*, vol. 54, pp. 2864–2873, 2007.

[12] Y. A. R. I. Mohamed and E. El-Saadany, "A current control scheme with an adaptive internal model for torque ripple minimization and robust current regulation in pmsm drive systems," *Energy Conversion, IEEE Transactions on*, vol. 23, pp. 92–100, 2008.

[13] H. Jin and J. M. Lee, "An rmrac current regulator for permanent-magnet synchronous motor based on statistical model interpretation," *Industrial Electronics, IEEE Transactions on*, vol. 56, pp. 169–177, 2009.

[14] J.-X. Xu, S. Panda, Y.-J. Pan, T.-H. Lee, and B. H. Lam, "A modular control scheme for pmsm speed control with pulsating torque minimization," *Industrial Electronics, IEEE Transactions on*, vol. 51, pp. 526–536, 2004.

[15] K. C. Yeo, G. Heins, and F. De Boer, "Comparison of torque estimators for pmsm," in *Power Engineering Conference, 2008. AUPEC '08. Australasian Universities*, 2008, pp. 1–6.

[16] K. J. Astrom and B. Wittenmark, *Adaptive Control*, 2nd ed. Boston, MA, USA: Addison-Wesley Longman Publishing Co., Inc., 1994.

[17] S. Sastry, *Nonlinear systems: analysis, stability, and control*. Springer New York, 1999, vol. 10.

[18] D. Schroeder, *Elektrische Antriebe - Regelung von Antriebssystemen*. Springer, 2009.

[19] O. Wallmark, "On control of permanent-magnet synchronous motors in hybrid-electric vehicle applications," Ph.D. dissertation, Chalmers University of Technology, 2004.

Qian Liu finished his Bachelor in Electrical Engineering in 2008 at Shanghai Jiao Tong University, China. In 2011 he received his Master degree in Control Engineering from Technical University of Kaiserslautern, Germany. Currently he is a research associate in the Institute of Electrical Machines at RWTH Aachen University, Germany. His research focuses on wind turbines, motor drive system and power electronics.

Andreas Thul received his master in electrical engineering at RWTH Aachen University in 2013. He is currently working as a research associate in the Institute of electrical Machines at RWTH Aachen University, Germany. His research focuses on electrical drive systems.

Kay Hameyer received his M.Sc. degree in electrical engineering from the University of Hannover and his Ph.D. degree from the Berlin University of Technology, Germany. After his university studies he worked with the Robert Bosch GmbH in Stuttgart, Germany as a Design Engineer for permanent magnet servo motors and vehicle board net components. Until 2004 Dr. Hameyer was a full Professor for Numerical Field Computations and Electrical Machines with the KU Leuven in Belgium. Since 2004, he is full professor and the director of the Institute of Electrical Machines (IEM) at RWTH Aachen University in Germany. 2006 he was vice dean of the faculty and from 2007 to 2009 he was the dean of the faculty of Electrical Engineering and Information Technology of RWTH Aachen University. His research interests are numerical field computation and optimization, the design and controls of electrical machines, in particular permanent magnet excited machines, induction machines and the design employing the methodology of virtual reality. Since several years Dr. Hameyers work is concerned with the development of magnetic levitation for drive

more then 250 journal publications, more then 300 international conference publications and author of 4 books. Dr. Hameyer is a member of VDE, IEEE senior member, fellow of the IET.